RIGA TECHNICAL UNIVERSITY
Faculty of Power and Electrical Engineering
Institute of Industrial Electronics and Electrical Engineering

Aivis Ašmanis
Doctoral Student of the Study Programme "Computerised Control of Electrical Technologies"

SURFACE-MOUNT COMPONENT 3D MODELLING IN FREQUENCY RANGE 150 KHZ−100 MHZ

Summary of the Doctoral Thesis

Scientific supervisor
Professor Dr. habil. sc. ing.
LEONĪDS RIBICKIS

RTU Press
Riga 2018

Ašmanis, A. Surface-mount Component 3D Modelling in Frequency Range 150 kHz−100 MHz.
Summary of the Doctoral Thesis. Riga: RTU Press, 2018. 36 p.

Printed in accordance with the decision of the Promotion Council "P-14" of 14 June , 2018, Minutes No. 2018-1 (63).

ISBN 978-9934-22-122-4 (print)
ISBN 978-9934-22-123-1 (pdf)

DOCTORAL THESIS PROPOSED TO RIGA TECHNICAL UNIVERSITY FOR THE PROMOTION TO THE SCIENTIFIC DEGREE OF DOCTOR OF ENGINEERING SCIENCES

To be granted the scientific degree of Doctor of Engineering Sciences, the present Doctoral Thesis has been submitted for the defence at the open meeting of RTU Promotion Council on 4 October 2018 at the Faculty of Power and Electrical Engineering of Riga Technical University, Āzenes iela 12/1.

OFFICIAL REVIEWERS

Professor Dr. habil. sc. ing. Oskars Krievs,
Riga Technical University.

Dr. sc. ing. Andris Mednis,
SIA "Mikrotīkls", Latvia

Professor Dr. sc. ing. Lauri Kütt,
Tallinn University of Technology, Estonia

DECLARATION OF ACADEMIC INTEGRITY

I hereby declare that the Doctoral Thesis submitted for the review to Riga Technical University for the promotion to the scientific degree of Doctor of Engineering Sciences is my own. I confirm that this Doctoral Thesis had not been submitted to any other university for the promotion to a scientific degree.

Name Surname ……. (signature)
Date: ……

The Doctoral Thesis has been written in Latvian. It consists of Introduction; 3 chapters; Conclusion; 146 figures; 15 tables; 2 appendices; the total number of pages is 172. The Bibliography contains 52 titles.

Contents

GENERAL DESCRIPTION OF THE THESIS

Topicality of the subject

European Union (EU) Electromagnetic Compatibility (EMC) Directive 2014/30/EU [1] provides that all electronic equipment sold in the EU market must comply with its requirements. Today's trend of electronics is an increase in operating speed and work frequency at the same time reducing size and weight. The result is a compact and light electronic device whose components are positioned very close to each other, leading to mutual coupling between components. As a component, the following text has been adopted to call an element that has a certain capacity − capacitors and an element with a certain inductance − inductance coil.

The electromagnetic interference (EMI) filters are applied in all electronic equipment, the basic task is to reduce the spread of conductivity and radiated interference. Following the trend of reducing the size of the electronics, the size and weight of the EMI filters are reduced by wide application of surface assembly components. Surface assembly components are inductance coils and capacitors, which are attached on PCB with the surface assembly technology. The mutual coupling between components depends heavily on the positioning of the components, the coupling increases by positioning the components closer to one another. Consequently, coupling and positioning of the surface assembly components on the PCB becomes a very important aspect of the design of filters.

Many studies [5], [12] have been carried out about the analysis of inductive and capacitative components of classical assembly, measuring of their parameters and measurement errors. Also an analysis of the EMI filter`s intercomponent mutual coupling with 3D electromagnetic field modelling tools has been carried out. However, there is a lack of information about the intercomponent mutual coupling of the surface assembly components in EMI filter, using 3D electromagnetic field modelling tools.

In the available studies [5], [20], [22], [26], [27] there mutual coupling analysis of classical assembly inductive components are described, but the studies have been carried out for unloaded components, through which current is not flowing, which can be variable in a real electronic system, depending on the working mode and load. In such variable-load current conditions the core material for inductive components may be saturated, it may change the electromagnetic field around components, which may affect the coupling of inductive components with other components or PCB tracks. Therefore it is essential to carry out a study on loaded inductive components by analysing the effects of the current on the parasitic

parameters of inductive components, it is necessary to establish a filter prototype BT for such studies. Performing a component loading with direct current, DC can enter the vector network analyser ports and permanently damage equipment. The following filters provide a load current in the measured component and ensure full DC insulation from the measurement ports. In addition, the filter must ensure the invariance of full resistance of the inductive component during measurements, which can be affected by a connected power source during measurements. The creation and optimisation of such filter will allow to carry out studies on loaded inductive components.

The aim and tasks of the research

The aim of the Doctoral Thesis is as follows: to carry out an analysis of mutual coupling between surface assembly inductive and capacitive components, depending on the interchangeability of components using a 3D electromagnetic field modelling tool. In order to achieve the aim of the Thesis the following tasks were defined.

1. To collect the latest scientific literature on the study of the parasitic coupling of surface assembly components and its innovations.
2. To research the methodology for measuring the parameters of the surface assembly components.
3. To perform surface assembly capacitor studies using 3D electromagnetic field modelling tools.
4. To perform surface assembly inductance studies using 3D electromagnetic field modelling tools:
    - two terminal inductive components;
    - four terminal inductive components.
5. To perform studies on mutual coupling between various surface assembly components using 3D electromagnetic field modelling tools.
6. To explore and perform high-frequency parameter improvement capabilities for surface assembly capacitors using 3D electromagnetic field modelling tools.
7. To develop a filter prototype using 3D electromagnetic field modelling tools. The filter is designed to measure the full resistance of the inductive components within a frequency range 150 kHz−100 MHz by entering direct current in a component.
8. To carry out a comparison and analysis of the performance parameters of a new filter prototype with equivalent commercially available filters.

Research methodology

In this Doctoral Thesis the author has applied the 3Delectromagnetic field modelling tool “Computer Simulation Technology Microwave Studio” (CST MWS), performed measurements with ZVRE-vector network analyzer, and compared the results using Matlab software.

The results and scientific novelty of the research

Systematic studies have been carried out for the new measuring methodology for the parasitic coupling on surface assembly components with the vector network analyser and improved mathematical calculations of error.

Original surface assembly capacitors and inductance 3D models were developed that allow to carry out the analysis of parasitic coupling with electromagnetic field modelling tools within a frequency range 150 kHz−100 MHz.

A new filter prototype was developed to measure the full resistance of the loaded inductive components within a frequency range of 150 kHz−100 MHz. The filter was optimized with the help of the 3D models, developed within this work, and electromagnetic field modelling tool CST MWS. The filter was developed and compared with equivalent commercially available scientific measurement filter. The new filter prototype has a higher permissible load current of 0.5 A, it can take measurements for a component with a full resistance less than 17 Ω, and an uncompensated inductive component is by 9 nH smaller. Therefore, the prototype of the filter is reasonably considered to be better.

Original 3D surface assembly capacitors and inductance models were developed to provide the possibility to analyse parasitic coupling between components with high accuracy.

Practical value of the research

The developed surface assembly capacitors and inductance 3D models allow carrying out the analysis of parasitic coupling effects on the performance of EMI filters in the frequency range 150 kHz−100 MHz. 3D models for surface assembly components have been developed based on the data provided by the component manufacturer. By applying the developed 3D models it is possible to save the cost and time of the EMI filter creation.

The developed 3D models of surface assembly components allow carrying out the analysis of parasitic coupling between components replacing time-consuming measurements

with expensive measuring equipment. 3D models of EMI filter components developed in electromagnetic field modelling tools are created based on the data − physical dimensions, material properties − provided by the component manufacturer. Therefore, the EMI filter and its effectiveness can be successfully analysed prior to the creation of a prototype without using expensive measuring equipment.

Approbation of research results

Results of the Doctoral Thesis were presented at 8 international conferences.

1. IEEE Asia-Pacific Symposium on Electromagnetic Compatibility, Singapore.
2. IEEE 58th International Scientific Conference on Power and Electrical Engineering of Riga Technical University (RTUCON), Riga, Latvia, 2017.
3. International Symposium on Electromagnetic Compatibility (EMC EUROPE 2017), Angers, France.
4. International Symposium on Electromagnetic Compatibility (EMC EUROPE 2016) Wroclaw, Poland.
5. ESA Workshop on Aerospace EMC (Aerospace EMC), Valencia, Spain, 2016.
6. 56th International Scientific Conference on Power and Electrical Engineering of Riga Technical University (RTUCON), Riga, Latvia, 2015.
7. IEEE International Symposium on Electromagnetic Compatibility (EMC Europa 2015), Dresden, Germany.
8. International Symposium on Electromagnetic Compatibility (EMC Europa 2014), Gothenburg, Sweden.

Results of the Doctoral Thesis are published in 11 publications.

1. **A. Asmanis**, G. Asmanis, D. Stepins, L. Ribickis, “3D Modelling and Analysis of Parasitic Couplings between Surface-Mount Components of EMI Filters", IEEE International Symposium on Electromagnetic Compatibility and IEEE Asia-Pacific Symposium on Electromagnetic Compatibility, Singapore, 2018, pp 1−6.

2. G. Džeriņš, **A. Asmanis**, G. Asmanis, A. Dzenis, “LED lighting equipment electromagnetic compatibility”, IEEE 58th International Scientific Conference on Power and Electrical Engineering of Riga Technical University (RTUCON), Riga, Latvia, 2017, pp 1−6.

3. **A. Asmanis**, D. Stepins, A. Dzenis, G. Asmanis ,“3D modelling of surface-mount capacitors and mutual couplings between them”, International Symposium on Electromagnetic Compatibility − EMC EUROPE, Angers, France, 2017, pp. 1-6.

4. **A. Asmanis**, G. Asmanis, D. Stepins, L. Ribickis, “Modelling of EMI filters with shields placed between the filter components”, International Symposium on Electromagnetic Compatibility − EMC EUROPE, Wroclaw, Poland, 2016, pp. 776−779.

5. **A. Asmanis**, G. Asmanis, D. Stepins, L. Ribickis, “High-frequency modelling of EMI filters considering parasitic mutual couplings”, ESA Workshop on Aerospace EMC (Aerospace EMC), Valencia, Spain, 2016, pp. 1−6.

6. G. Asmanis, L. Ribickis, D. Stepins, **A. Asmanis,** “Differential mode Π-type EMI filter modelling using CST MWS”, 56th International Scientific Conference on Power and Electrical Engineering of Riga Technical University (RTUCON), Riga, Latvia, 2015, pp. 1−5.

7. G. Asmanis, D. Stepins, **A. Asmanis**, L. Ribickis, “Mutual couplings between EMI filter components”, IEEE International Symposium on Electromagnetic Compatibility (EMC), Dresden, Germany, 2015, pp. 908–913.

8. G. Asmanis, D. Stepins, L. Ribickis, **A. Asmanis**,“Modelling of mutual coupling between inductors”, IEEE Symposium on Electromagnetic Compatibility and Signal Integrity, Silicon Valley, USA, 2015, pp. 294–299.

9. G. Asmanis, D. Stepins, **A. Asmanis**, L. Ribickis, “Capacitors mutual inductance modelling and reduction”, International Symposium on Electromagnetic Compatibility, Gothenburg, Sweden, 2014, pp. 1176–1181.

10. G. Asmanis, **A. Asmanis**, D. Stepins,“Mutual couplings in three phase T-type EMI filters”, International Symposium on Electromagnetic Compatibility − EMC EUROPE, Roma, Italy, 2012, pp. 1−6.

11. G. Asmanis, **A. Asmanis**, L. Ribickis, “Analysis of high frequency effects in three phase EMI filters”, Asia-Pacific Symposium on Electromagnetic Compatibility, Singapore, 2012, pp. 653–656.

DETAILED DESCRIPTION OF CHAPTERS

1. Characterisation of EMI filters and analysis of measurement methodology

In this chapter the author studies the methodology for the characterisation and measurement of the EMI filter and the mathematical analysis of the error.

EMI filter is characterised by the attenuation measured in decibels − dB, additional characters are the full resistance of the load and full resistance of the source. Filter attenuation depends on frequency, load and source resistance, and current. In industry EMI filters are not described entirely, because the full resistance of the load and source is dependent on frequency and varies according to frequency. For characterisation of the EMI filter scattering parameters (S-parameters) can be used, which provide the possibility to describe the filter attenuation at any full resistance of the source and load in wide range of frequencies. Using scattering parameters for filter characterization the filter is perceived as a two-port network, enabling the filter to be analysed with transmission and reflection coefficients. This type of filter analysis enables to use an indirect measurement for the determination of the filter`s parasitic parameters, which can be expressed from simplified equivalent circuits. Scattering parameters can be measured with a vector network analyser, using mathematical calculations to determine the full resistance of filters and components. There are three measurement methods for using the vector network analyser (Fig. 1.1).

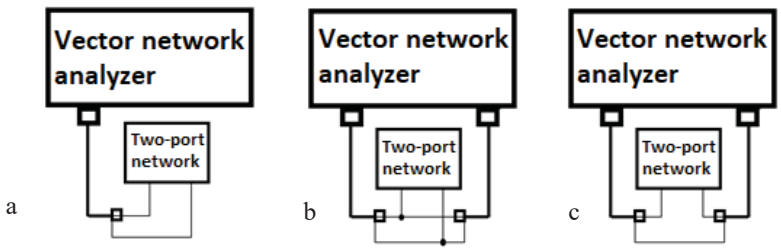

Fig. 1.1. Methods for measuring capacitor and inductive component via VNA.

1. Measurement of the reflection coefficient (*S*11) using one VNA port (Fig. 1.1. a).
2. Measurement of the forward transmission coefficient (*S*21) using both VNA ports connected in parallel (Fig. 1.1. b).

3. Measurement of forward transmission coefficient (*S*21) using both VNA ports connected in series (Fig. 1.1. c).

Each method introduces a measurement error that depends on both, component parameters and the frequency range in which measurements are taken.

a) The method works better if | *Z*11 | is close to 50 Ω. In this case, the reflection coefficient | *S*11 | will be significantly less than 0 dB.
b) The method works better if | *Z*11 | is less than 10 Ω. In this case, the transmission coefficient value | *S*21 | will be significantly less than 0 dB.
c) The method works better if | *Z*11 | is greater than 100 Ω. In this case, the transmission factor | *S*21 | will be significantly less than 0 dB.

For the capacitor measurements within the frequency range 100 kHz−500 MHz the most appropriate method is to connect the capacitor in parallel to the measurement ports (method b), as the full resistance of the capacitor in MHz range is below 10 Ω.

For the measurements of inductive components in frequency range 100 kHz−500 MHz the most appropriate method is to connect components into a series of measuring ports (method c), because the full resistance *Z*11 of the inductive component in the MHz range is greater than 100 Ω.

2. Development and verification of 3D models of surface assembly components

2.1 Development and verification of the 3D models of surface assembly capacitive components

In this subchapter the author describes the 3D model of the surface assembly capacitive components created with accuracy in a satisfactory combination with its simplicity (Fig. 2.1). For the 3D model the capacitor`s capacity and the series resistance are defined as a surface with dispersed parameters between two terminals of the capacitor.

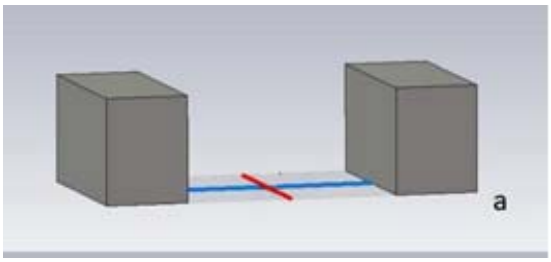

Fig. 2.1. 3D capacitor model is positioned in parallel to the leading surfaces of the capacitor using the distributed parameter surface.

In the sub-chapter, the author presents a voluminous study carried out on the methodology for measuring the surface assembly capacitor, and it has come to the knowledge that the measurement of the reflection coefficient (S11) using one VNA port is applied to determine the capacitor's capacity, but the measurement of the forward transmission coefficient (S21) using both VNA ports in parallel (Fig. 1.1. b) is applicable when it is essential to determine the accuracy of the equivalent value of series resistance of the capacitor and equivalent value of series inductance.

The developed 3D capacitor models have been verified through prototype measurements and modelling.

The developed 3D models have been used in parasitic couplings studies of surface assembly capacitors. When capacitors are located at a small distance from one another, their parasitic couplings appear. Parasitic couplings may be capacitive and inductive. If the capacitors are not positioned within a distance of millimetres, the inductive couplings component is dominated by parasitic couplings − M. Coupling between two capacitors with capacity C and

equivalent series resistance ESR is possible because of the equivalent series inductance ESL of capacitors.

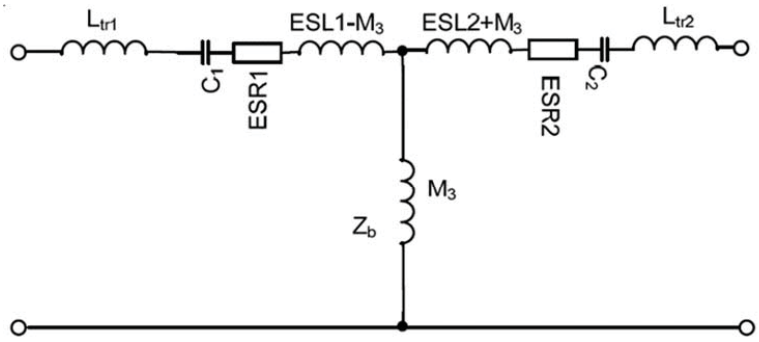

Fig. 2.2. Equivalent scheme for parasitic couplings between two capacitors.

A two-capacitor connection can be converted into an equivalent scheme as shown in Fig. 2.2. From this equivalent scheme, by expressing the full resistance shoulder Z_b, it is possible to determine the parasitic couplings M with expression (2.1).

$$M_3 = \left| Im\left(\frac{100S_{21}}{1 - S_{22} + S_{22}S_{11} - S_{11} - S_{21}^2} \right) \right| \frac{1}{2\pi f} \quad . \tag{2.1.}$$

CST MWS modelling results coincide with prototype measurements when the precision of 3Dsurface assembly capacitors` models is verified.

2.2 Development and verification of the 3D models of surface assembly inductive components

In this subchapter the author presents the creation of several 3D models for various surface assembly inductive components, and their error adjustment calculations to improve the accuracy of modelling results.

For the component WE 74279141 a 3D model has been created with an internal structure where *S*-parameter values are integrated (Fig. 2.3). The internal structure requires additional computing capacity, however the internal structure can play a crucial role in forecasting the precision of the parasitic couplings.

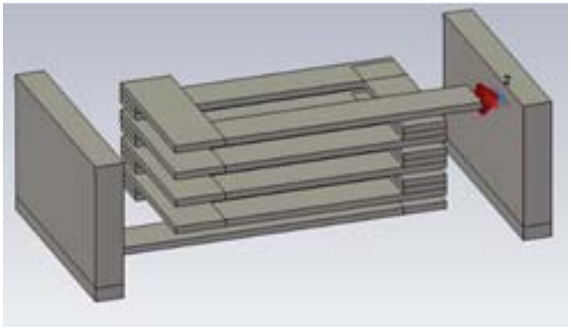

Fig. 2.3. 3D model of inductive surface assembly component WE 74279141 with an internal structure where *S*-parametric values are integrated.

The 3D model of the inductive component WE 744066151 − a partially shielded surface assembly component with a single core and winding − is designed with a precise internal structure (Fig. 2.4).

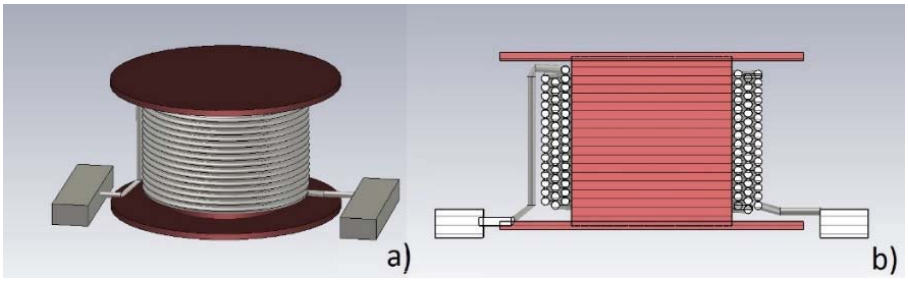

Fig. 2.4. 3D model of surface assembly component WE 744066151: a) 3D model of a component without an external core; b) cross-section of the 3D model without an external core.

In an inductive component WE 7447709471, which is a fully shielded surface assembly component with a separate core and winding, the 3D model is designed with a precise internal structure (Fig. 2.5).

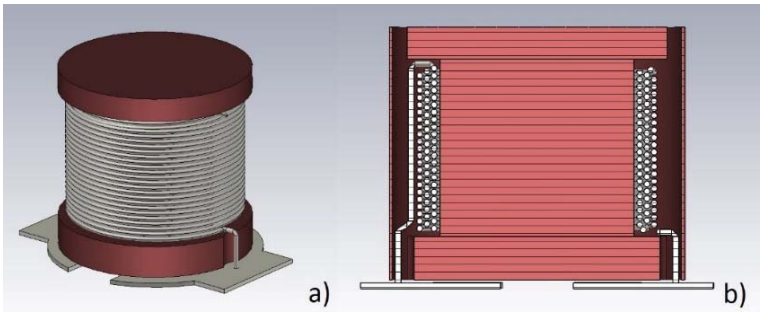

Fig. 2.5. 3D model of surface assembly component WE 7447709471: a) 3D model of the component without an external core; b) cross section of the 3D model.

The comparison of the full resistance measurement of inductive components and the calculation of analytical 3Delectromagnetic model is shown in Fig. 2.6. The 3D model of inductive component WE 74279141 has high accuracy, the model of the inductive components WE 744066151 and WE 7447709471 has satisfactory accuracy, above the resonance frequency results of calculations are lower than measurement results indicating that the inductance of the analytical 3D model is slightly higher than the inductance of the component, however the equivalent parallel capacity is significantly lower than the one of the real component.

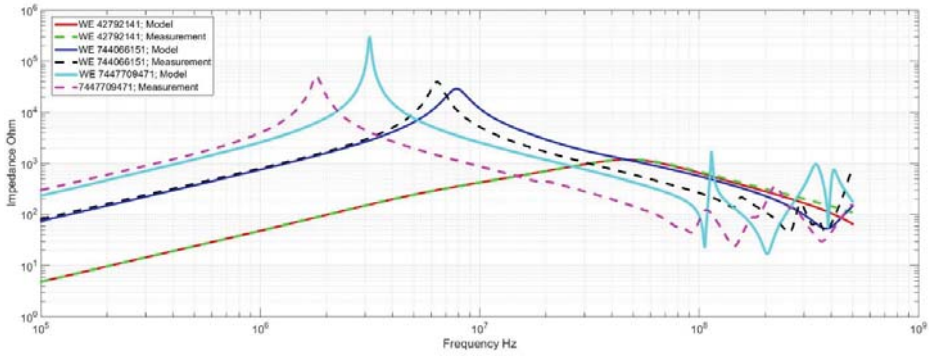

Fig. 2.6. Comparison of the full resistance calculation of the inductive component measurements and analytical 3D electromagnetic models.

In the studies of parasitic coupling between two surface assembly inductions the developed 3D models are used. The two-induction connection can be converted into the T-equivalent scheme from which with indirect path measurements it is possible to calculate the parasitic coupling M3. The T-equivalent scheme is given in Fig. 2.7.

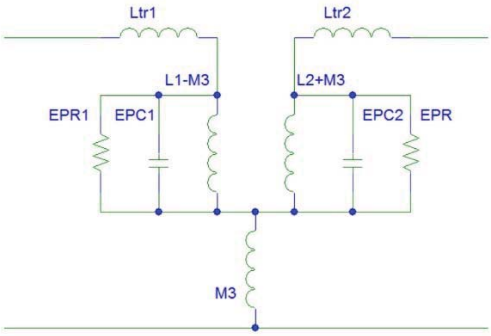

Fig. 2.7. The T-equivalent scheme for parasitic coupling between two inductions.

The third shoulder of T-equivalent scheme plays the most important role in parasitic coupling calculation because it includes coupling M3. Parasitic coupling M3 can be calculated by a relationship (2.2).

$$M_3 = \left| Im\left(\frac{100 S_{21}}{1 - S_{22} + S_{22} S_{11} - S_{11} - S_{21}^2} \right) \right| \frac{1}{2\pi f} \tag{2.2.}$$

The author has carried out analytical calculations using 3D models of all three combinations of inductive components to analyse mutual coupling, these results are compared with the prototype measurements.

Analytical calculations and measurements of the mutual coupling between surface assembly inductions show that the accuracy of the developed 3D model of surface assembly inductions is 2 dB–10 dB in the frequency range 2 MHz−100 MHz, whereas in the frequencies range below 2 MHz it is difficult to analyse, because of the noise level of VNA.

Based on the developed analytical 3D models, it is possible to quantify mutual coupling between surface assembly inductive components with a satisfactory accuracy.

2.3 Development and verification of the 3D models of inductive surface assembly components of four terminals

EMI filters use not only two terminal inductive components, but also four and six terminal components. Four terminal inductive components are the inductance coils for the reduction of

common mode (CM) and differential mode (DM) noise. The author performed *S*-parameters measurement for four terminal inductive components using the two-port VNA. Performing six different combinations of *S*-parameter measurements it is possible to get a matrix of resulting S-parameters that fully characterises the object of the research – four terminal components (2.3).

$$\begin{bmatrix} b_1 \\ b_2 \\ b_3 \\ b_4 \end{bmatrix} = \begin{bmatrix} S_{11} & S_{12} & S_{13} & S_{14} \\ S_{21} & S_{22} & S_{23} & S_{24} \\ S_{31} & S_{32} & S_{33} & S_{34} \\ S_{41} & S_{42} & S_{43} & S_{44} \end{bmatrix} \begin{bmatrix} b_1 \\ b_2 \\ b_3 \\ b_4 \end{bmatrix} = [S] \begin{bmatrix} a_1 \\ a_2 \\ a_3 \\ a_4 \end{bmatrix} \tag{2.3}$$

When integrating this S-parameter matrix into the 3D four terminal inductive component, a precise 3D model can be obtained (Fig. 2.8), which describes the properties of the properties of four terminal inductive component common mode (CM) and differential mode (DM).

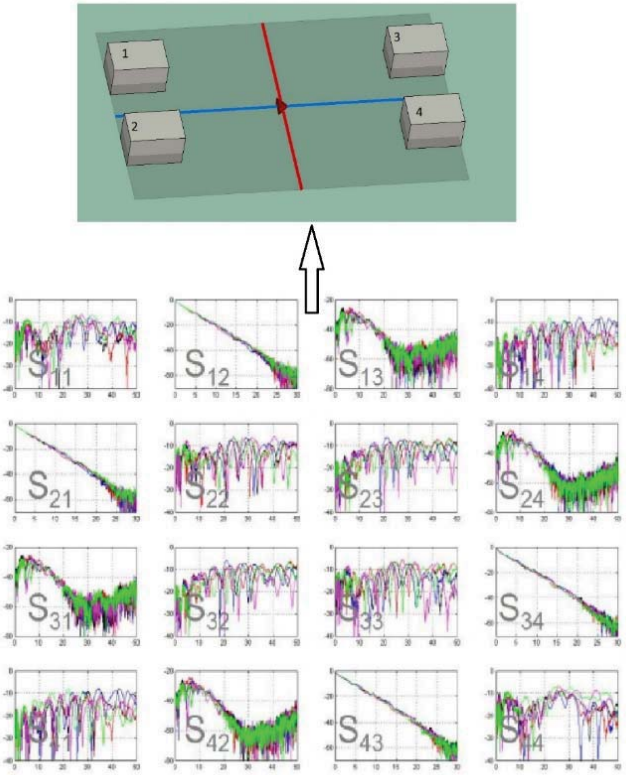

Fig. 2.8. 3D model of a four terminal inductive surface assembly component with integrated *S*-parametric values.

In order to improve the measurement of *S*-parameters of the four terminal inductive components, a mathematical base for the adjustments of the results is established, thus enabling the improvement of accuracy of the results.

The developed 3D models have been tested and verified by prototype measurements. As a result of analytical calculations it is possible to calculate the full resistance of the component and CM inductance with high accuracy. DM inductance is relatively small, so the accuracy of its calculations is poor.

2.4 Improving high frequency parameters for surface assembly capacitors

Shunt condenser connecting signal track and PCB GND is a low-cost effective high-frequency filter used in many areas. The performance of the shunt surface assembly capacitors in a high-frequency range is limited not only by the equivalent series inductance of capacitors, but also by parasitic coupling between the input and output of the capacitors circuit, leading to a capacitor inductive nature above its resonance frequency [38], [1], [40], [41].

Such deficiencies may be avoided by means of constructive solutions, minimizing the length and height of the PCB tracks above the grounded plane connected to the condenser through the interlayer transition [40], [42]. In order to further improve the performance of the shunt condenser filter, it is necessary to use methods that compensate for the parasitic inductance of the shunt condenser [43] − [48]. However, these parasitic inductance schemes are designed for physically large capacitors that are usually used in large power systems. In paper [39] a new method has been presented, which successfully suited [44] condenser filters for the reimbursement of parasitic inductance.

This method allows to offset the parasitic inductance of the shunt capacitors using magnetic interaction between single plane tracks. The results [39] show that the effective offsetting of the parasitic inductance of the shunt capacitors via surface assembly technology can be achieved at the expense of the filter size increase.

3. Filter prototype development

In the third chapter the author presents the development and optimisation of the filter operating at a frequency range 150 kHz−100 MHz by applying in the optimised process the 3D models of surface assembly component described in the second chapter. Such filters are required for measurements of inductive components to assess the effects of magnetic material saturation depending on load current, which can change the component`s full resistance. It is also possible to use such a filter for measurements of EMI filters to determine the effect of the current on the filter attenuation.

The prototype filter is intended to provide a load current >1A. A replaceable DC load current is provided from the DC power supply that will flow only through the inductive components. The filters will ensure that the DC current does not flow into the analyser entrances that can damage it. Therefore the filter must ensure full DC insulation from the VNA ports, if the power voltage does not exceed 50 V.

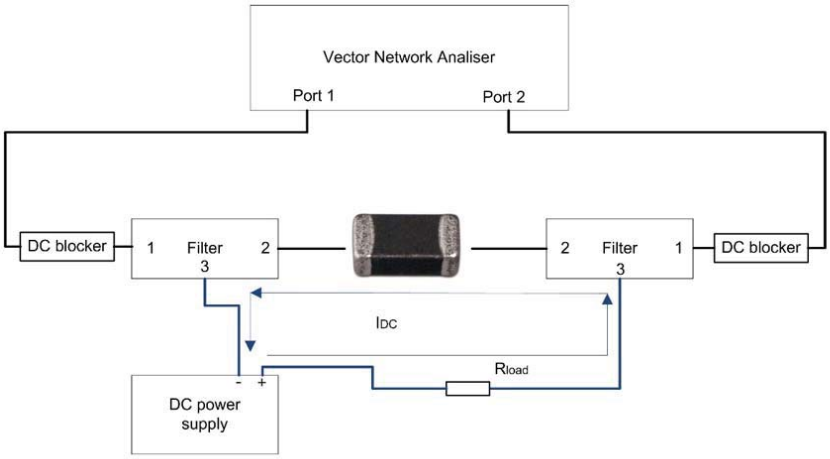

Fig. 3.1. Filter use flowchart.

The filter prototype must ensure that the resistance of the inductive component is not altered because of the additionally connected circuits and the power supply unit. The filter provides measurements for the inductive components within a frequency range 150 kHz−100 MHz in which the full resistance of components may exceed 1.5 kΩ. The filter must have a negligible effect on the results of the measurements, so that precise measurements of the inductive component are provided.

The requirements for the filter prototype are as follows:

- to ensure the current of 1A (between ports 2−3);
- to ensure the isolation of the DC-voltage (for port 1);
- transmission coefficient S12 and S21 < 0.5 dB;
- reflection coefficient S11 and S22 < −25 dB;
- transmission coefficient S13 < −25 dB.

The basic component for creating a prototype filter is inductive components, whose parameters define the filter parameters throughout all frequency range. Wurth Electronik surface assembly inductive components have been selected for the creation of a prototype. All components have been subjected to measurements and adjustments according to the method of adjustment of the measurements developed by this study. Full resistance measurements of the components have been carried out in shielded chamber to obtain high accuracy measurements without the environmental impact of the surrounding electromagnetic environment. Surface assembly inductive components may be divided into two parts.

1. EMI inductive components, which are designed to filter interference with low benefits and therefore resonance with high amplitude. Such components do not require parallel connected resistance for resonance reduction, as such is ensured by the design of the inductive component itself.
2. Inductive components are designed for the accumulation of the magnetic energy. These components are characterised by low losses, high benefits and expressed resonance of the full resistance that need to be damped in parallel with resistance.

Calculation of inductance of discarded inductive components is given in Fig. 3.2.

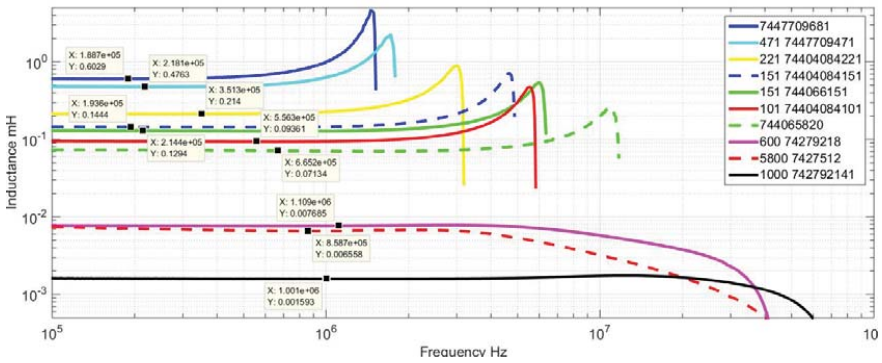

Fig. 3.2. Results of inductance calculations of surface assembly inductive components.

For a filter-defined frequency range of 150 kHz-100MHz it is necessary to select the components that evenly cover the entire range of frequencies ensuring a steady attenuation throughout the frequency range, whereas one inductive component is unable to ensure that, so several inductive components are to be applied. Components with high inductance provide high resistance in a low frequency range, however above the full resistance resonance frequency dominant parallel parasitic capacity of the component, which reduces resistance. Low-frequency components provide low resistance in the low frequency range, however they also have a far lower parallel parasitic capacity, providing higher resistance in the high frequency range than components with high inductance.

Four inductive components − WE 1000_742792141, WE 600_74279218, WE 151_744066151, WE 471_7447709471 − are used for the creation of a prototype.

Based on the methodology and analytical 3D models described in the previous chapter, an optimised filter scheme (Fig. 3.3. a) has been established, for which an analytical calculation of the S -parameters with CST MWS has been performed. Parameters calculated on the analytical path meet the requirements of the filter.

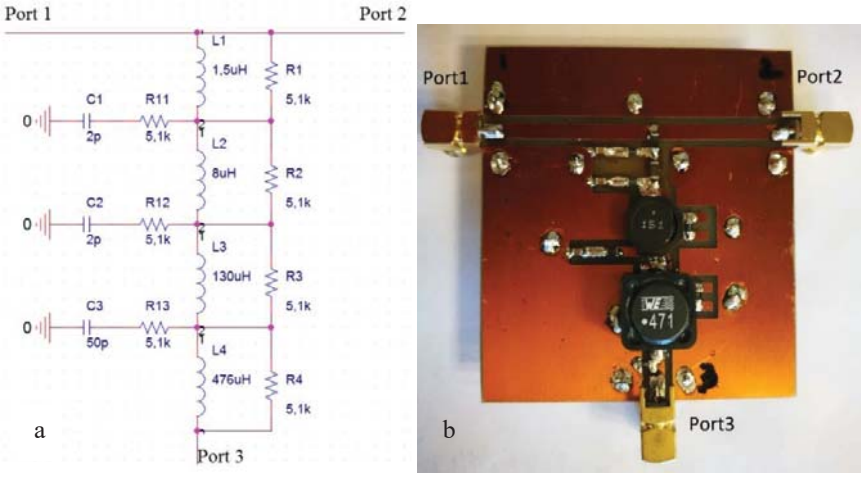

Fig. 3.3. Filter prototype:
a) scheme; b) filter prototype PCB with components.

Based on the developed scheme (Fig. 3.3) a filter prototype has been created (Fig. 3.3. b) for the measurement of the S-parameters. Comparison of the analytical and measurement results of the filter prototype is given in Figs. 3.4−3.6.

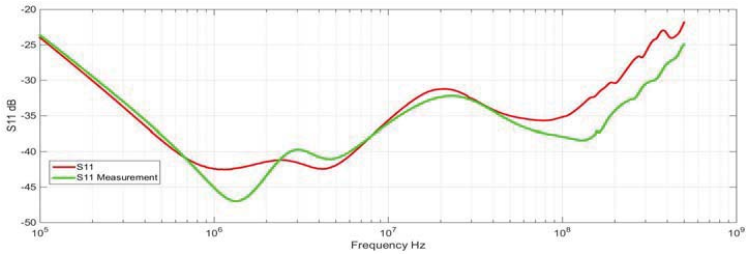

Fig. 3.4. Comparison of the analytical and measurement results of Port 1 of the filter prototype.

The values of the measured reflection coefficient S11 coincide with the analytical calculations of 5 dB accuracy (Fig. 3.4). The results show that the value of the reflection coefficient is below −25 dB in the range of 150 kHz−100 MHz.

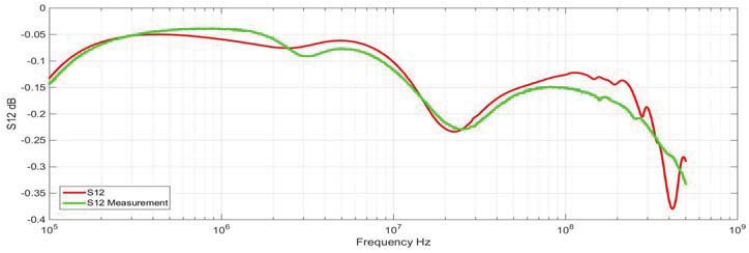

Fig. 3.5. Comparison of the analytical and measurement results of Ports 1−2 of the filter prototype transmission coefficient *S*12.

The measured transmission coefficient values *S*21 coincide with analytical calculations with an accuracy of < 0.1 dB (Fig. 3.5). The results show that the transmission coefficient values *S*21 are below 0.5 dB in a frequency range of 150 kHz−100 MHz.

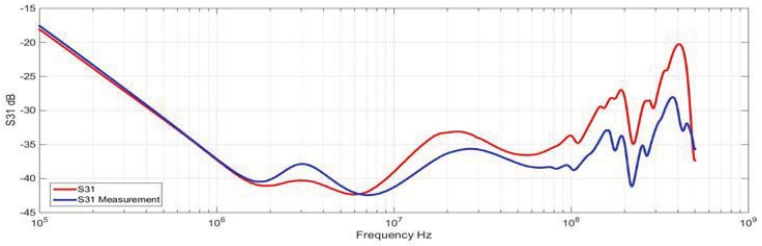

Fig. 3.6. Filter prototype transmission coefficient *S*31 between Ports 3−1; comparison of analytical calculations and measurements.

The measured prototype transmission coefficient *S*31 coincides with analytical calculations in the frequency range up to 10 MHz (Fig. 3.6). In the frequency range 10 MHz−100 MHz, results coincidence is within 8 dB. The measurement results are above −25 dB and theoretically do not meet the assigned task. However, if the measurement was carried out in real conditions, when the port resistance was < 1 Ω, the *S*31 would be substantially lower and the assignment would be fulfilled.

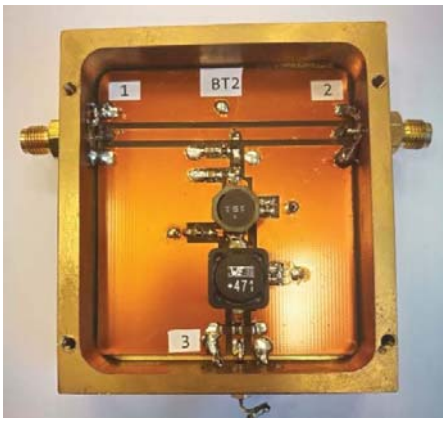

Fig. 3.7. Filter prototype with enclosure.

The full functioning of the prototype requires the enclosure to perform screening functions and ensure the reference surface (reference plane) as well as structural rigidity for the assembly of SMA connectors for correct measurements. The enclosure is made of brass. Images of the enclosure and filter prototype are given in (BT1) Fig. 3.7. The filter image does not include the cover of the filter enclosure. The enclosure is covered at the time of the measurement. According to the measurement methodology (Fig. 3.1), two identical filters are required for the measurements of the inductive components, so two identical filters BT1 and BT2 have been produced.

The GND layer of PCB plate of the filter is put in contact with the enclosure and the outer layer of the SMA connectors is attached to the GND layer of PCB. BT1 and BT2 with a PCB, whose GND layer is connected to the enclosure, produce 22 nH inductive components and 0.58 pF capacitive components. This inductive component shall be taken into account when measurements are taken for SMD components with very low resistance. The inductive component 22 nH generates 13.8 Ω in addition to resistance at 100MHz. Such additional

resistance does not significantly affect the measurements of inductive and capacitive components.

For measurements of inductive components in the methodology, flowchart (Fig. 3.1) has external DC component locking circuits (DC-blocker BLK-89-S+ with a working range of up to 50 V), the DC flows only through Port 3, however it does not flow through the BT1 and BT2 enclosures. In this situation the BT1 and BT2 enclosures are isolated from DC that could cause problems in the higher frequency range due to uncertainty caused by the parasitic capacity between the enclosure, PCB and components.

In scientific studies, filters are used when measuring the parameters of the inductive components by changing the component load current. Such filters are widely available in the market, but for a limited range of frequencies. The current is limited to 0.5 A. For example, study [51] uses Mini Circuits ZFBT-4R2GW+. This study does not have to analyse the ZFBT-4R2GW+ effects on measurements results. The measurement adjustment is assumed to be perfect and ZFBT-4R2GW+ will not influence the results of the measurements. An analogous assumption is also made regarding the impact of the load current on measurements. In order to analyse the quality of this study and impact of filter ZFBT-4R2GW+ on the measurement, filters ZFBT-4R2GW+ were purchased and measurements performed. The results of the measurement of the S-parameters have been compared with the developed filter prototypes BT1 and BT2. Filter ZFBT-4R2GW+ images and internal structure are given in Fig. 3.8.

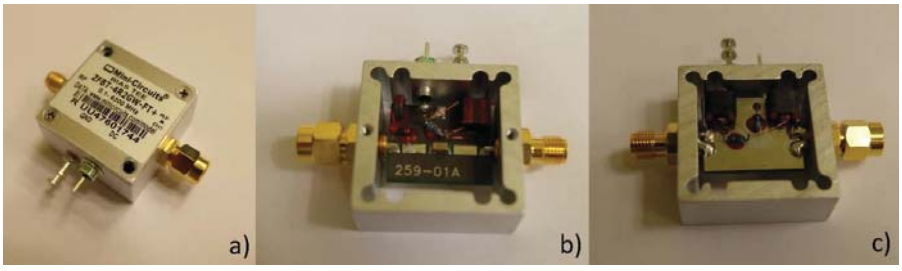

Fig. 3.8. Filter ZFBT-4R2GW+:
a) front view; b) front view without cover; c) rear view without cover.

Comparison of S-parameter measurements for ZFBT-4R2GW+ with developed filters BT is given in Figs. 3.9 and 3.10. Reflection coefficient of filter ZFBT-4R2GW+ (Fig. 3.8) is very similar (within 5 dB), which shows good repeatability of parameters from filter to filter. Compared to BT filter the reflection coefficient for ZFBT-4R2GW+ is higher in the frequency

range 0.1 MHz−10 MHz. In the frequency range of 10 MHz−70 MHz, reflection coefficients are higher for BT filter. For both types of filters reflection coefficient resonances are observed, when the frequency exceeds 100 MHz.

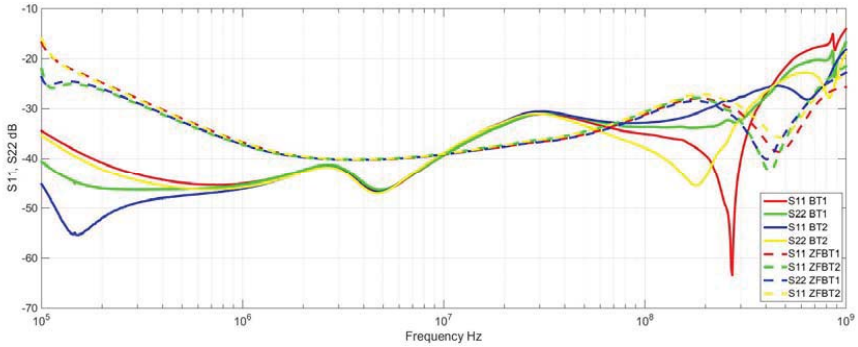

Fig. 3.9. Measurement of reflection coefficient for filters BT and ZFBT-4R2GW+.

The transmission coefficient S21 values for filter ZFBT-4R2GW+ are compared with the filter BT transmission coefficient in Fig. 3.10. Filter BT transmission coefficient values within the range from 0.1 MHz to 100 MHz are higher than −0.4 dB. Filter ZFBT-4R2GW+ transmission coefficient values reach −1.1 dB at the beginning of the frequency range near 10 MHz.

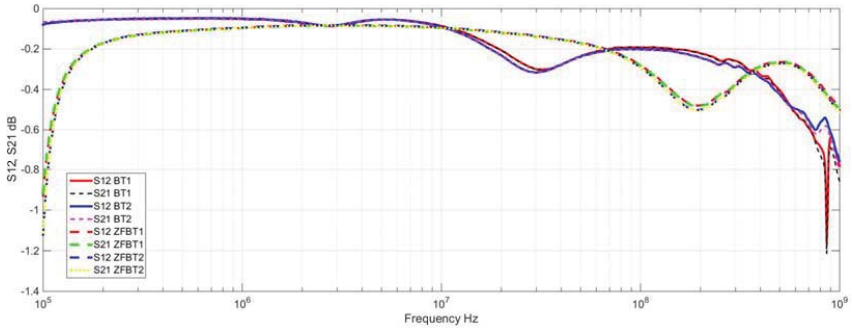

Fig. 3.10. Measurements of the transmission coefficient for filters BT and ZFBT-4R2GW+.

In order to compare the performance of filter ZFBT-4R2GW+ with the performance of filter BT, measurements (Fig. 3.11) have been carried out using the schematic shown in Fig. 3.1. Measurements have been carried out with PCB simulating short-circuit (small impedance) and a PCB on which the resistance of 1 Ω, 1 k Ω and inductive components L1 WE 42 792141 and L2 WE 742 782 18 is mounted. Measurements have been carried out with DC current

0 A, 0.2 A. Measurements with DC current 0.5 A have not been performed, because the limitation current of filter ZFBT-4R2GW+ is 0.5A and it could be damaged. The measurement adjustment has been made. Measurements have been compared with filter BT measurements and direct measurements carried out using only VNA.

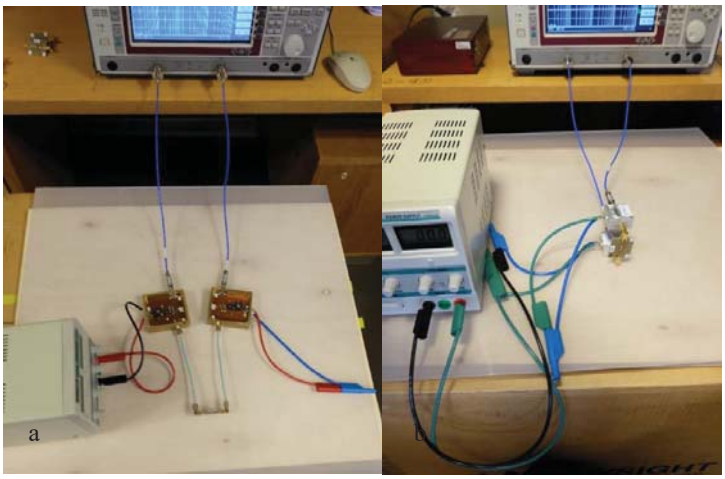

Fig. 3.11. PCB measurements:
a) filter prototype BT; b) commercial filter ZFBT-4R2GW+.

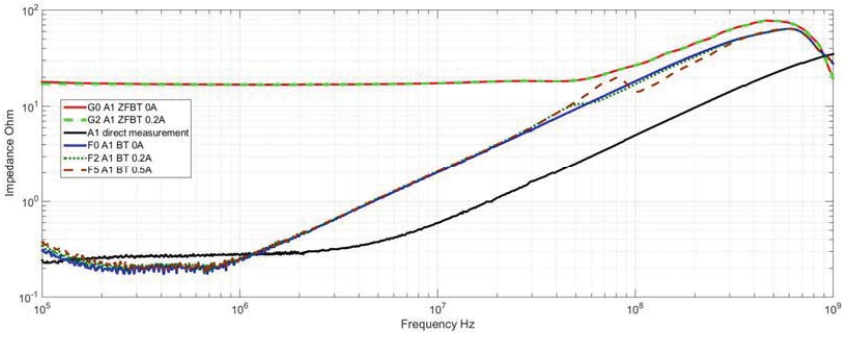

Fig. 3.12. Short-circuit PCB measurements using ZFBT-4R2GW+ compared to BT measurements.

Analyses of measurements with PCB simulating short-circuit in Fig. 3.12 makes it possible to see that the measurements taken with filter ZFBT-4R2GW+ vary significantly from filter BT measurements and direct measurements using VNA in the frequency range up to 70MHz. With filter ZFBT-4R2GW+ it is not possible to take measurements below 17 Ω. Also,

the non-compensated inductive component of series is larger than in the case with filter BT, it reaches 36 nH. With filter BT, the series inductive component is 27 nH, but by direct measurements it is 7.7 nH. The DC current does not have an impact on the results of filter ZFBT-4R2GW+ measurements.

PCB with mounted 1 Ω resistor measurements are shown in Fig. 3.13. These measurements also confirm that measurements taken with ZFBT-4R2GW+ cannot be below 17 Ω.

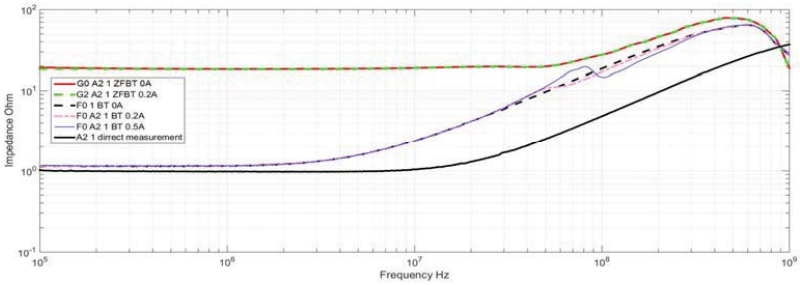

Fig. 3.13. Comparison of PCB A2 resistance measurements with 1 Ω using filter ZFBT-4R2GW+ and BT measurements.

PCB with 1 k Ω measurements is given in Fig. 3.14. In the frequency range up to 70 MHz the filter ZFBT-4R2GW+ and filter BT measurements are within 10 Ω. Filter BT measurements above 70 MHz are closer to direct measurements using only VNA. This is due to non-compensated capacitate components, using filter ZFBT-4R2GW+ this component is greater than in the case of filter BT. In the frequency range between 0.1 MHz and 100 MHz measurements with filters BT and ZFBT-4R2GW+ are very close to direct measurements using only VNA.

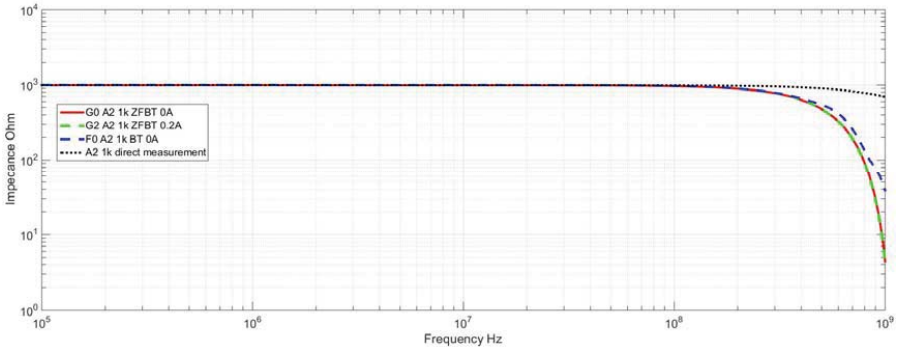

Fig. 3.14. PCB A2 with 1 k Ω resistance measurements compared to BT measurements.

Measurements of the inductive components are shown in Figs. 3.15. and 3.16. Measurements using filter ZFBT-4R2GW+ are similar with the measurements taken with filter BT.

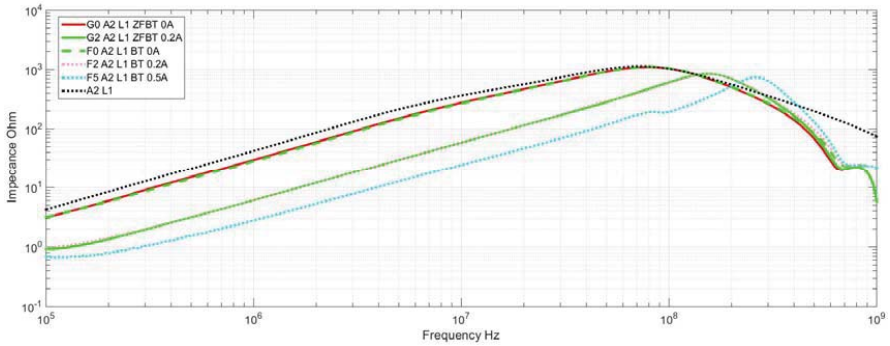

Fig. 3.15. Comparison of measurements of PCB A2 with inductive component L1 WE 42 792 141 and BT measurements.

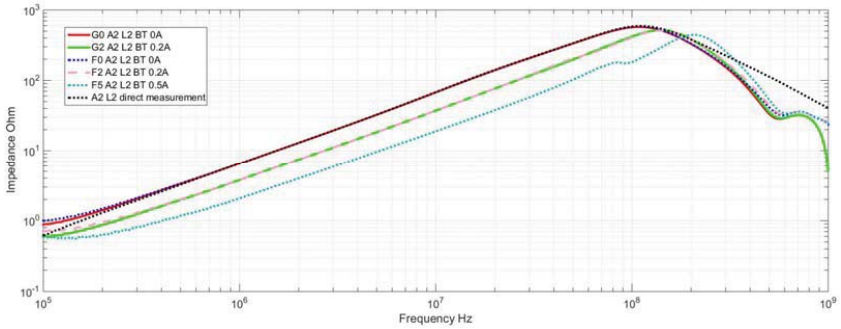

Fig. 3.16. Comparison of measurements of PCB A2 with inductive component L2 WE 742 782 18 and BT measurements.

Assessing all the results it can be concluded that created filters BT have significantly better parameters and provide more benefits than filter ZFBT-4R2GW+ used in the scientific research [51]. Filter BT can make significantly lower resistance measurements and uncompensated series inductance is lower than in the case with filter ZFBT-4R2GW+. Filter BT is capable of providing a large DC current. One of the shortcoming of filter BT is the need to use coaxial cables to connect the measured object.

Conclusions

Original surface assembly capacitors and inductance 3D models were developed and can be used in the electromagnetic field modelling tool CST MW to analyse the parasitic coupling between components within a frequency range of 150 kHz−100 MHz. The 3D models are optimized in order to reduce the requirement for computing resources and increase the accuracy of models prediction. The developed 3D models have been verified by prototype measurements using a vector network analyser. The original 3D models have been successfully applied in the creation of a new filter prototype designed for full resistance measurements of loaded inductive components. The developed filter prototype is compared with an equivalent filter ZFBT-4R2GW+ available in the market and the analysis of the results was performed.

Full resistance values of the developed 3D surface assembly capacitor models compared to the taken prototype measurements are with < 2.2 % error, regardless of used measurement method and the position of the SMA connector. Parasitic coupling between surface assembly capacitors is insignificant (between 0.3 nH and 0.045 nH), however in the frequency range above 100 MHz, it can play an essential role in providing at least 40 dB links between decoupled circuits. At frequencies 1 GHz there is a 25 dB parasitic link from the capacitor parasitic coupling. Parasitic coupling can be calculated on an analytical path without measurement with a 30 % error, if the capacitors are more than 1 mm away from each other. For capacitors within 1 mm from each other the parasitic coupling reduction error is only 14 %.

The difference of the full resistance analytical calculations with prototype measurements for the developed 3D surface assembly inductors (ferrite bead inductors) models is negligible: < 1 % in the frequency range below 100 MHz, which is the base study frequency range for this work, however in the frequency range above 100 MHz the difference is < 10 %. Shielded surface assembly inductor 3D models full resistance characteristic coincide with prototype measurements till the resonance frequency for the component WE 7447709471 with ~ 2 % error and WE 744066151 with ~ 4 % error. This means that the inductive component of 3D model has been correctly calculated with an acceptable accuracy of the error, but equivalent parallel capacity has been calculated inaccurately, errors for both components exceeding 7 %. The errors of 3D models are explained by unknown ferromagnetic material properties and complexity of the component`s internal structure.

Analytical calculations and measurements of parasitic coupling show that the coupling between the surface assembly inductions can be determined with the accuracy of 2 dB–10 dB in frequency range between 2 MHz and 100 MHz. Frequency range below 2 MHz starts VNA noise level, so it is not objective to compare the results.

Four terminal inductive components can be measured using a two port VNA. *S*-parameter measurements can be integrated into four terminal inductive components 3D model, which enables including the characteristics of the CM and DM inductive component in a single analytical model. With analytical 3D models it is possible to calculate inductive component`s full resistance and CM inductance with high accuracy.

It is possible to reduce parasitic parameters of the surface assembly capacitors by simple variation of the location of capacitors, allowing to reduce effects of mutual coupling in high frequency range. With varying variations of PCB tracks, it impossible to obtain a compensatory mutual coupling and increase capacitors resonance frequency.

In the third chapter a filter prototype for BT is presented developed with electromagnetic field modelling tool. The filter is intended for the measuring full resistance of loaded inductive component. The following filter requirements are defined:

- to ensure the current of 1A (between Ports 2−3);
- to ensure the isolation of DC-voltage (for Port 1);
- transmission coefficient S12 and S21 < 0.5 dB;
- reflection coefficient S11 and S22 < −25 dB;
- transmission coefficient S13 < −25 dB.

Development of filter prototype BT designed and optimized with component 3D models is presented in the second chapter. After a successful application of electromagnetic field modelling tool CST MW in the filter optimization, the pre-defined filter requirements are reached and tested with real prototype measurements.

The developed filter prototype BT is compared with commercially available filter equivalent ZFBT-4R2GW+. The comparison is based on vector network analyser measurements for PCB with 1 Ω, 1 k Ω and inductive components L1 (WE 42 792141) and L2 (WE 742 782 18), additionally inductive components are measured with DC current 0 A, 0.2 A

load. Measurement results are processed with measurement adjustment expressions. By analysing the data it may be concluded that:

- filter BT causes the un-compensated 22 nH inductive components and 0.58 pF capacitive components, but commercially available filter ZFBT-4R2GW+ causes 36 nH inductive components and 0.74 pF capacitive components;
- maximum permissible current of filter BT is 1A, but of filter ZFBT-4R2GW+ it is 0.5 A;
- filter ZFBT-4R2GW+ is unable to perform measurements, if the full resistance of the measured component is lower than 17 Ω, but filter BT is able to measure under 17 Ω;
- In the frequency range up to 70 MHz the measurements of filter ZFBT-4R2GW+ and filter BT are within 10 Ω difference.

Therefore it can be concluded that the developed filter BT prototype has better parameters than the commercially available filter equivalent ZFBT-4R2GW+.

The objective of the Doctoral Thesis has been reached and tasks have been fulfilled. The developed original EMI filter 3D models can be considered an industry novelty, thay allow accurate analysis of parasitic coupling effects on EMI filter performance efficiency. 3D models are designed to reduce the computational resource and time requirements.

Continuation of work

The Doctoral Thesis covers only part of the necessary studies on modelling a complete EMI filter with the electromagnetic field modelling tool CST MSW.

Further studies are intended to be devoted to the following tasks:

- development of merger filter prototypes BT in one enclosure;
- study on loaded surface assembly inductance with the electromagnetic field modelling tool CST MSW;
- improvement of the precision of 3D models within a frequency range of 150 kHz−500 MHz;
- Complete single-phase filter modelling with electromagnetic field modelling tool CST MSW.

BIBLIOGRAPHY

[1] EIROPAS PARLAMENTA UN PADOMES DIREKTĪVA 2014/30/ES (2014. gada 26. februāris) par dalībvalstu tiesību aktu saskaņošanu attiecībā uz elektromagnētisko savietojamību).

[2] "MIL-STD-220C:2009, Military standart: Method of insertion loss measurement".

[3] "CISPR 17:2011 Methods of measurement of the suppression characteristics of passive EMC filtering device".

[4] K. Kurokawa, "Power Waves and the Scattering Matrix," IEEE Transactions on Microwave Therory and Techniques, Vol. 2, No. 13, pp. 194−202, 1965.

[5] G. Asmanis, "Measurament and modelling of EMI filters high frequency parasitic parametrs," PhD thesis, Rīga, 2014.

[6] D. P. Newkirk, U. L. Rohde, "RF/Microwave Circuit Design for Wireless Applications," London: Wiley-Interscience, 2000, p. 920.

[7] Kenneth L. Kaiser, "Electromagnetic Compatibility Handbook," Florida: CRS press, 2005, p. 2568.

[8] S. Wang, F. C. Lee, W. G. Odendaal, "Using scattaring parametrs to characterize EMI filters," Power electronics specialists' conference, 2004, PESC, 2004, pp. 297−303.

[9] Kye Yak See and Junhong Deng, "Measurement of noise source impendance of SMPS using a two probes approach," IEEE Transactions on Power Electronics, Vol. 19, No. 3, pp. 862−868, 2004.

[10] V. Tarateeraseth, Bo Ho, Kye See, and F.G. Canavero, "Accurate Extraction of Noise Source Impedance of an SMAP Under Operating Conditions," IEEE Transactions on Power Electronics, Vol. 25, No. 1, pp. 111−117, 2010.

[11] Lee Smith, Jeff Gruszynski Dick Anderson. (1996, November) Test & Measurement Application Note 95-1 S-Parameter Techniques. Hewlett Packard.

[12] G. Asmanis, A. Asmanis, D. Stepins, "Measuring capacitor parametrs using vector network analyzers," Electronics, Vol. 18, No. 1, pp. 29−38, 2014.

[13] Ultra low impendence measurements using 2-port measuraments, Agilent application note., 2004, p. 52.

[14] R. Dosoudil. “Determination of permeability from impedance measurement using vector network analyzer,” Journal of electrical engineering, Vol. 63, No. 7, pp. 94−96, 2012.

[15] G. Ghione, M. Pirola, “Microwave Electronics,” Cambridge University Press, pp. 96, 2017.

[16] http://katalog.we-online.com/en/pbs

[17] https://en.wikipedia.org/wiki/Ceramic_capacitor

[18] R. P. Deshpande “Capacitors: Technology and Trends,” Tata McGraw-Hill Education, 2012, pp. 319.

[19] CST microwave studio workflow & solver overview. : CST, 2016, p. 127.

[20] A. Asmanis, D. Stepins, A. Dzenis, G. Asmanis, “3D Modelling of Surface-Mount Capacitors and Mutual Couplings Between Them,” EMC EUROPE 2017, Angers, France, September 4−8, 2017.

[21] R&S Test and Measurement Division, “Vector network analyser,” p. 322.

[22] I. F. Kovacevic, T. Friedli, A. M. Musing, J. W. Kolar, "3-D Electromagnetic Modelling of Parasitics and Mutual Coupling in EMI Filters," IEEE Trans. on Power Electronics, Vol. 29, No. 1, pp. 135−149, 2014.

[23] S. Wang, Lee, F. C., Odendaal W. G., “Characterization and parasitic extraction of EMI filters using scattering parameters,” IEEE Transactions on Power Electronics, Vol. 20, No. 2, pp. 502–510, March 2005.

[24] R&S Test and Measurement Division, “Vector Network Analyzer (VNA) Calibration: The Basics,” p. 10.

[25] Agilent “De-embedding and Embedding S-Parameter Networks Using a Vector Network Analyzer,” Application Note 1364-1, May 30, 2004, p. 24.

[26] G. Asmanis, D. Stepins, L. Ribickis, A. Asmanis, “Modelling of Mutual Coupling between Inductors,” Proc. of IEEE Symposium on Electromagnetic Compatibility and Signal Integrity, USA, Santa Clara, 15−20 March, 2015, pp. 294−299.

[27] A. Asmanis, D. Stepins, G. Asmanis, L. Ribickis, “3D Modelling and Analysis of Parasitic Couplings between Surface-Mount Components of EMI Filters,” 2018 IEEE International Symposium on Electromagnetic Compatibility and 2018 IEEE Asia-Pacific Symposium on Electromagnetic Compatibility, Singapore, 2018, pp. 1–6.

[28] A. B. Meniüa-nin, M. S. Damnjanoviü, Lj. D. Živanov. “MODELLING OF EMI FILTERS WITH SHIELDS PLACED BETWEEN THE FILTER COMPONENTS”, 7th International Symposium on Intelligent Systems and Informatics. Serbia, Subotica, 25−26 Sept., 2009, pp. 77−80.

[29] V. Zhurbenko, “Advanced Microwave Circuits and Systems”, 2010.

[30] Würth Electronics “Trilogy of Magnetics“, 4th edition, 2012, p. 700.

[31] J. Frei, Xiao-Ding Cai, S. Muller, “Multiport S-Parameter and T-Parameter Conversion With Symmetry Extension”, IEEE TRANSACTIONS ON MICROWAVE THEORY AND TECHNIQUES, Vol. 56, No. 11, 2008, pp. 2493–2504.

[32] M. Salter, “4 port VNA versus 2 port VNA: A comparison of methods for measuring the S parameters of a directional coupler”, 4th European ANAMET Seminar METAS, Bern, Switzerland, 3 June 2015.

[33] D. G. Kam, J. Kim, “Multiport Measurement Method Using a Two-Port Network Analyzer With Remaining Ports Unterminated” IEEE Microwave and Wireless Components Letters, Vol. 17 (I9), 2007, pp. 694−696.

[34] A. Asmanis, G. Asmanis, D. Stepins un L. Ribickis, “High-frequency modelling of EMI filters considering parasitic mutual couplings”, ESA Workshop on Aerospace EMC (Aerospace EMC), Valencia, Spain, 2016.

[35] G. Asmanis, A. Asmanis un D. Stepins, “Modelling of EMI filters with shields placed between the filter components”, International Symposium on Electromagnetic Compatibility − EMC EUROPE, Wroclaw, Poland, 2016.

[36] G. Asmanis, L. Ribickis, D. Stepins un A. Asmanis, “Differential mode Π-type EMI filter modelling using CST MWS”, -, Riga, Latvia, 2015.

[37] I. F. Kovačević, T. Friedli, A. M. Müsing un J. W. Kolar, “3-D Electromagnetic Modelling of Parasitics and Mutual Coupling in EMI Filters”, IEEE Transactions on Power Electronics, Vol. 29 (1), pp. 135−149, 2014.

[38] T. Zeeff, T. Hubing, T. Van Doren, D. Pommerenke, “Analysis of simple two capacitor low pass filters”, IEEE Trans. Electromagnetic Compatibility, pp. 595–601, 2003.

[39] J. McDowell, T. Hubing, “Parasitic Inductance Cancellation for Surface Mount Shunt Capacitor Filters”, IEEE Transaction of Electromagnetic Compatibility, pp. 74–82, 2014.

[40] G. Tang, “Surface mount capacitor loop inductance calculation and minimization”, IEEE International Symposium on Electromagnetic Compatibility, 1998.

[41] C. N. Olsen, T. Van Doren, T. Hubing, J. Drewniak, R. DuBroff, “Improving the high-frequency attenuation of shunt capacitor, low-pass filters”, IEEE International Symposium on Electromagnetic Compatibility, 13−17 Augut 2001.

[42] E. Bogatin, Signal and Power Integrity-Simplified, NJ: Engelwood Cliffs, 2004.

[43] T. Neugebauer, J. Phinney un D. Perreault, “Filters and components with inductance cancellation”, IEEE Transactions on Industry Applications, Vol. 40 (2), pp. 483−491, 2004.

[44] T. Neugebauer, D. Perreault, “Filters with inductance cancellation using printed circuit board transformers”, IEEE Transactions on Power Electronics, Vol. 19 (3), pp. 591−602, 2004.

[45] F. L. W. O. S. Wang, “Cancellation of capacitor parasitic parameters for noise reduction application”, IEEE Transactions on Power Electronics, Vol. 21, No. 4, 2006.

[46] B. Pierquet, T. Neugebauer, D. Perreault, “A Fabrication Method for Integrated Filter Elements With Inductance Cancellation”, IEEE Transaction Power Electronics, pp. 838–848, 2009.

[47] H.-F. Chen, C.-Y. Yeh, un K.-H. Lin, “A Method of Using Two Equivalent Negative Inductances to Reduce Parasitic Inductances of a Three-Capacitor EMI Filter”, IEEE Transactions on Power Electronics, Vol. 24, No. 12, pp. 2867−2872, 2009.

[48] B. J. Pierquet, T. C. Neugebauer, D. J. Perreault, “Inductance Compensation of Multiple Capacitors With Application to Common- and Differential-Mode Filters”, IEEE Transactions on Power Electronics, Vol. 21, No. 6, pp. 1815−1824, 2006.

[49] J. Bernal, M. Freire, S. Ramiro, “Simple and cost-effective method for improving the high frequency performance of surface-mount shunt capacitors filters”, IEEE International Symposium on Electromagnetic Compatibility (EMC), Dresden, 2015.

[50] Clayton R. Paul, “Introduction to Electromagnetic Compatibility, 2nd ed. London: Wiley-Interscience, 2006.

[51] Čedo J. Žlebič, Dragan R. Kljajić, Nelu V. Blaž, Ljiljana D. Živanov, Aleksandar B. Menićanin, Mirjana S. Damnjanović, “Influence of DC Bias on the Electrical Characteristics of SMD Inductors” IEEE Transactions on Magnetics, 2015, Vol. 51, (1).

[52] EN 55032- Electromagnetic compatibility of multimedia equipment − Emission Requirements.